GeoVirtual 2020 September 14-16 Resilience and Innovation

Mechanical behavior of a shallowly buried steel pipe during compaction procedure

Yadong Zhang, Ron Chik-Kwong Wong
Department of Civil Engineering – University of Calgary, Calgary, Alberta, Canada

ABSTRACT
A steel pipe (Grade X52) of 0.6 m in diameter and 5.2 m in length was buried in a soil pit formed by three reinforced concrete walls and a curved masonry wall. The pipe was instrumented with strain gauges mounted externally at two pipe sections to measure both circumferential and longitudinal deformations. The mechanical behavior of the buried pipe was monitored throughout the compaction. The circumferential strains were generally higher than the longitudinal strains along the pipe axis. The upper and lower parts of the pipe were under tension and compression, respectively. The absolute strain values increased with the initial soil compaction up to the pipe crown level, then decreased when the backfill was compacted above the pipe. The curvature of the lower pipe ring increased, while the pipe crown was more curved compared to the initial circular shape. The pipe was deformed into an inverted "Y" shape.

RÉSUMÉ
Un tuyau en acier (Grade X52) de 0,6 m de diamètre et de 5,2 m de longueur a été enterré dans une fosse de sol rigide formée de trois murs en béton armé et d'un mur de maçonnerie incurvé. Le tuyau a été instrumenté avec des jauges de contrainte montées à l'extérieur sur deux sections de tuyau pour mesurer les déformations circonférentielles et longitudinales. Le comportement mécanique du tuyau enterré a été suivi durant le compactage. Les déformations circonférentielles étaient généralement plus élevées que celles le long de la longueur du tuyau. Les parties supérieure et inférieure du tuyau sont respectivement sous tension et compression. Les valeurs de déformation absolue ont augmenté initialement avec le compactage jusqu'au niveau du sommet du tuyau, puis ont diminué en raison du compactage du sol au-dessus du tuyau. Le tuyau a été déformé en forme de «Y» inversé.

1 INTRODUCTION

Steel pipelines have been widely used in oil and gas industry. According to Alberta Energy Regulator (2013), total length of 415,152 km pipelines have been built in Alberta, Canada, among which 86% are made of steel. Steel pipe is usually classified as flexible and allowed to deform (5% of pipe diameter) under internal and/or external loads.

Compared to rigid pipes, flexible pipes deform at a higher magnitude under soil and/or external loads, because of the low stiffness. Because of this, the soil column above the flexible pipe moves downward with the friction at sides pointing upward. Therefore, the load transferred to the pipe is minimized by the amount taken by the frictional force. This is also known as the "positive" arching effect named by Terzaghi (1943). In addition, the installation procedure was found to play a predominant role in the pipe behavior under surface loading (Chapman et al. 2007). The significance of this effect varies with soil type and compaction quality of sidefill as well as backfill. The nomenclatures "sidefill" and "backfill" are used to define the soil below and above the pipe top level, respectively.

Firstly, the magnitude of pipe deflection depends on compaction quality. Nielson (1972) experimentally investigated the impact of compacted soil density on pipe deflection. A 6% increment of sand density resulted in a decrease of 90% in pipe deflection at the same overburden. Later Moghaddas et al. (2011) found that when the relative density of sand increased from 42% to 57%, the final deflection of HDPE (high-density polyethylene) pipe was decreased by half under repeated point load.

Secondly, the installation procedure also influences the sign (positive or negative) of pipe deflection. The widely used Iowa formula derived by Spangler (1938) is based on the assumption that the horizontal pipe diameter increases while the vertical one decreases for buried flexible pipes. However, it has been

experimentally illustrated that the vertical diameter was elongated when the flexible pipe was buried in heavily compacted sand or gravel. For example, laboratory results on a corrugated steel pipe reflect that the vertical diameter increased due to the initial backfilling up to pipe crown, then this effect was reduced by continuous backfilling above the pipe (Lay 2012). However, at the end of backfilling with a cover depth of 0.9 m, the vertical diameter was still larger than the initial value. Similar behaviors were detected in PVC (polyvinyl chloride) (Sargand et al. 1995), uPVC (unplasticized polyvinyl chloride) (Rogers 1988) and HDPE (Rogers et al. 1995) pipes.

Finally, the deformed shape of pipe is also affected by the installation procedure. Spangler (1938) assumed that the pipe deformed into an ellipse with vertical contraction and horizontal elongation. Howard (1972) investigated the deformed shape of flexible pipes under surface surcharge. These flexible pipes were found either deformed into an “elliptical” (Figure 1 (a)) or a “rectangular” shape (Figure 1 (b)), depending on the relative stiffness ratio between the pipe and the surrounding soil. Rogers (1988) further introduced two more types of deformation, i.e., the “heart” (Figure 1 (c)) and inverted “heart” (Figure 1 (d)) shaped deformations, based on the experimental results on shallowly buried uPVC pipes. The deformed shapes could be deduced by the pipe-wall strain profile.

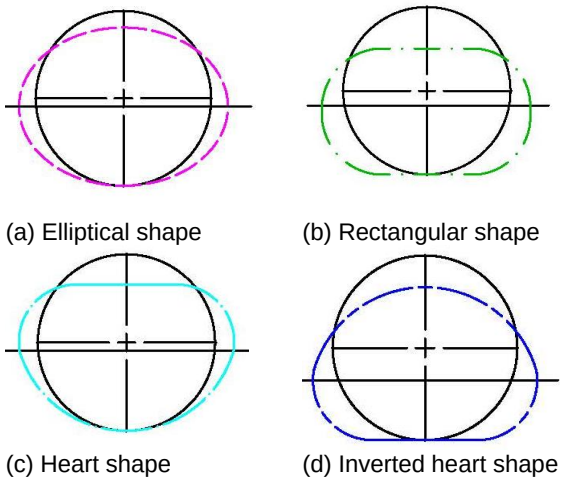

Figure 1. Different types of pipe deformation (after Rogers (1988))

However, very limited researches have been done to investigate the behavior of plain steel pipe throughout the whole process of compaction, particularly for large diameter pipe with a shallow burial depth. In this study, a full-scale test on a 0.6 m diameter steel pipe was conducted in the Structures High Bay Laboratory at University of Calgary. The external strains at two sections were continuously measured during backfilling. The development of deformed pipe shape with compaction was captured based on the pipe-wall strain profiles.

2 MATERIAL PROPERTIES

A 5.2 m long section of X52 steel pipe (approximate 970 kg weight) was instrumented and then buried in a soil pit. The outer diameter and wall thickness of the pipe are 0.6 m and 12.7 mm, respectively. The length to diameter ratio is 8.6, while the diameter to thickness is 48. Material parameters of this steel are presented in Table 1.

The soil material used as backfill was obtained from a construction site nearby the university campus. The standard Proctor maximum dry density was determined to be 1976 kg.m^{-3} at an optimum moisture content of 13.5%. Figure 2 presents the particle size distribution curve, with estimated C_c and C_u coefficients of 0.80 and 4.72 based on the distribution curve, respectively. PL and LL were experimentally determined to be 16.7% and 21.9%, respectively. Therefore the soil is classified as silty sand or SM according to the Unified Soil Classification System ASTM D2487-11 (2017). This type of soil is listed and recommended by CSA (2014) for structural material. The moisture content of the native soil is about 12%, corresponding to 97.6% of the Proctor maximum dry density. Therefore, during backfilling the soil was compacted without any water addition.

Table 1. Physical and mechanical parameters of X52 steel

Parameter	Unit	Value
ρ	kg.m^{-3}	7,800
E	GPa	206
v	-	0.3
σ_y	MPa	360
σ_t	MPa	455

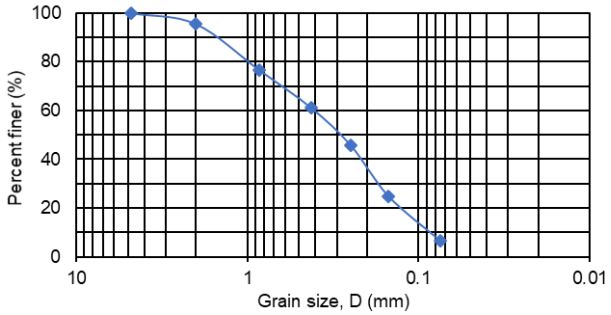

Figure 2. Particle size distribution curve of the soil material

3 EXPERIMENTAL SETUP AND INSTRUMENTATIONS

The test steel pipe section was buried in a soil pit built in the Structures High Bay Laboratory at University of Calgary. The pit was formed by three reinforced concrete walls and a curved masonry wall as shown in Figure 3. The dimensions of the pit are 7.6 m (length) by 2.4 m (width in the middle) by 2.4 m (height). The curved wall

is symmetrical about its middle length. The narrowest and widest widths of the pit are 2.4 m and 3.8 m, respectively. The ratio of the minimum pit width to the pipe diameter is 4, which is larger than 3.3 as used and recommended by Brachman et al. (2008) in their experiments on flexible pipes.

Two pipe sections (Sections A and B shown in Figure 3) were externally instrumented with general purpose tee gauges of CEA-06-250UT-350 series. These sections are symmetrical about the pipe centerline, and 1.8 m away from each other, which is the center-to-center distance of the two tires at the same axle of CL-W truck (CSA 2014). For this 350 Ohms resistance gauge, the strain range is ±5% at the temperature range between -75°C and +175°C. The advantage of using this gauge is that it could measure strains in two perpendicular directions (90°) simultaneously as shown in Figure 4. Because of this fact, each tee gauge was taken as two uniaxial strain gauges perpendicular to each other. The uniaxial strain gauges in odd and even numbers measured strains along the circumference and the pipe axis, respectively. In addition, the temperature effect is self-compensated for this type of gauge. At each section, eight tee gauges were mounted from the pipe crown with 45° intervals as shown in Figure 5. These gauges were connected to a data acquisition system which has the capability of handling all 48 cables. The pipe ends were closed after instrumentation by pressurized plywood to prevent soil migration into the pipe (the cables were run along the pipe wall inside the pipe).

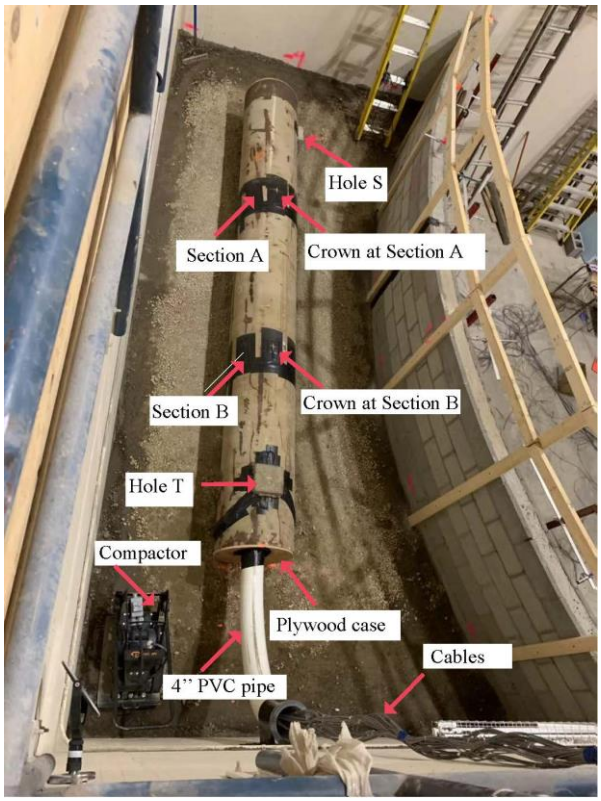

Figure 3. Experimental layout with pipe sitting above uncompacted granular bedding

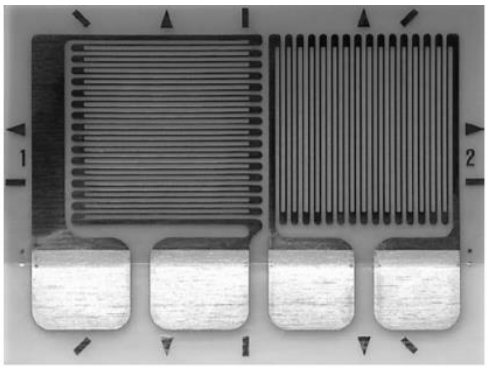

Figure 4. CEA-06-250UT-350 general purpose tee rosette gauge

To investigate any potential impact of the masonry wall on the behavior of the soil-pipe system, the deflection of the masonry wall was monitored during the compaction procedure. The deflection was deduced by analysing the pictures taken by an ultra-high speed laser scanner produced by Leica Geosystems AG during the installation and compaction procedures.

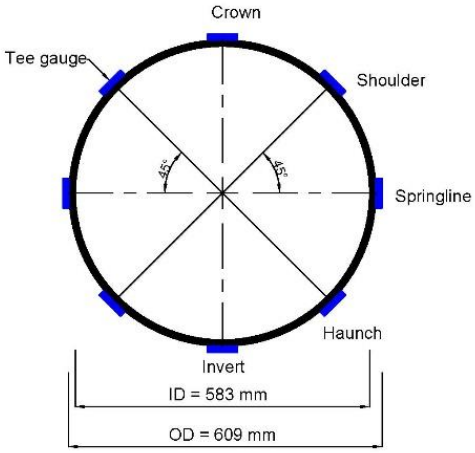

Figure 5. Cross-sectional sketch showing instrumentation at Sections A and B

4 TEST PROCEDURE

The installation procedure was carried out in the order as follows:

(1) Emplacing the soil and compacting it to the height of 0.9 m from the concrete pit base;
(2) Spreading a 200 mm layer of loose granular soil as specified by CSA (2014) and then installing the pipe above it;

(3) Continuing placing and compacting the sidefill and backfill to the final designed height of 2.3 m. Therefore, the final depth of cover is 0.6 m.

The vertical distance from the soil pit base to the pipe invert is almost twice of the pipe diameter, which is considered as sufficient to eliminate the effect from the concrete base of the soil pit (Lay and Brachman 2014). The bedding is considered as a trench bottom and designed to be 1.2 m wide to meet the minimum requirement of twice the outer diameter for steel pipes (CSA 2014).

An electrical plate compactor produced by Packer Brothers Inc. was used for the soil compaction as presented in Figure 3. The plate is 0.6 m long and 0.43 m wide, with an estimated contact pressure of 57 kPa. Soil was compacted in layers to a bulk density no less than 95% of the standard Proctor density with a thickness not exceeding 200 mm. As shown in Figure 6, soil densities measured at different heights are all larger than 95% of the maximum dry density. The measured density of the compacted soil below the pipe is higher than that above it. However, the variation is only less than 1% at the interval above the bedding. Therefore, for the sidefill and backfill, the compaction quality is considered uniformly distributed along the height. In such doing, the compaction quality of backfill meets the requirements based on both American and Canadian design codes (American Iron and Steel Institute. Highway Task Force 2007, CSA 2014).

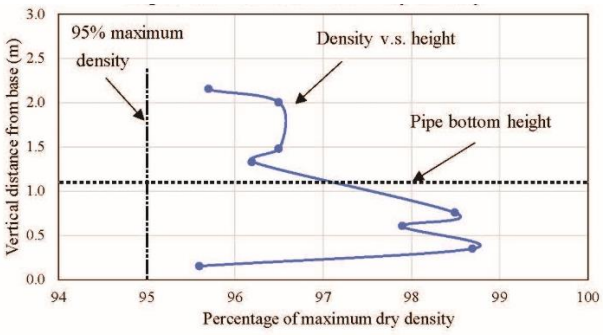

Figure 6. Soil relative density versus height from the concrete base of the soil pit based on neutron logging

To have a full picture of pipe deformation behavior throughout the installation procedure, strain measurements were started before emplacing and compacting of the first layer of sidefill above the bedding. The whole backfilling procedure was finished in 10 layers with each not exceeding 200 mm in thickness. The vertical distances from pipe invert were recorded after compacting each layer and listed in Table 2. Special care was taken to guarantee the compaction quality of the soil at pipe sides. Therefore, the sidefill was split into 6 layers with the maximum thickness of 150 mm for a single layer. The final depth of cover was reached after 10 layers at 0.6 m (equal to the pipe diameter), which is the minimum depth of cover required for this type of pipe (AASHTO 1999, CSA 2014).

Table 2. Details of compaction layers

Layer #	Vertical distance from pipe invert (m)
1	0.15
2	0.3
3	0.35
4	0.43
5	0.5
6	0.6 (pipe crown level)
7	0.75
8	0.9
9	1.05
10	1.2 (final depth of cover = 0.6 m)

5 RESULTS AND DISCUSSION

The behavior of the masonry wall was analyzed firstly to evaluate the performance of the soil pit. The outward deflection of the wall was found increasing with height due to the soil load and energy input from compactor. However, the maximum value, among the eight monitored locations along the top of the masonry wall, was only 2.5 mm. Therefore, the wall is considered as rigid and has only very limited impact on the pipe-soil system.

5.1 Strain versus Height of Compaction

In Figure 7, the circumferential and longitudinal strains at pipe crown are plotted with respect to the heights from the invert. The strains measured at the crown are the highest along the circumference. Gauges 5 and 6 were mounted at Section A, with gauges 21 and 22 at Section B. The vertical dashed line represents the level of pipe crown or the completion of layer 6. Positive strain values represent the case that the gauge is under tension, and vice versa.

Along both directions, the strains measured at the two sections were close to each other throughout the compaction. This demonstrates the relatively uniform distribution of compaction quality along the pipe length.

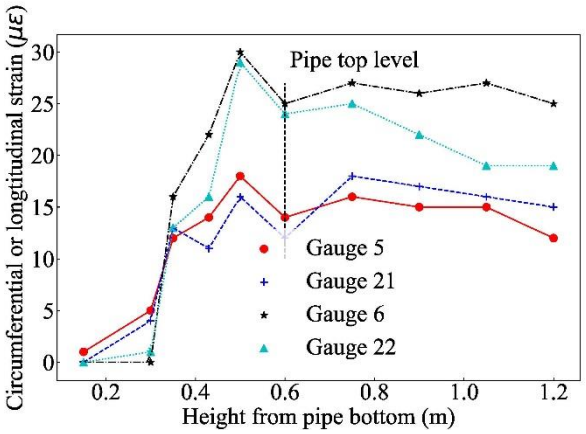

Figure 7. Relation between compaction height and strains at pipe crown of Sections A and B

The circumferential strain was larger than that along the pipe axis, particularly when the soil was compacted above the springlines. The circumferential to longitudinal strain ratio is between 1.2 and 2.1 with an average of 1.65, which means the circumferential stress is more significant at the crown.

The circumferential and longitudinal strains were increased with compaction to the height of 0.5 m from pipe invert, then decreased when placing and compacting the soil above the pipe. This is referred to as the so-called 'Peaking effect' that the maximum tensile strains and vertical elongation are reached when the soil is compacted to the crown level, because of the lateral soil pressure induced by the compactor and the soil material placed at both sides of the pipe (McGrath et al. 1999, Masada and Sargand 2007). Advantage could be taken from this effect to minimize the pipe deformation caused by higher backfill and external surcharge, for example, truck load. This effect is most significant for shallowly buried flexible pipes like the one in this research, because pipe takes most of the truck load as it is stiffer than the surrounding soil. In addition, the maximum readings during the compaction are much smaller than that at yielding (1700 με). Therefore, no performance limit was caused by the installation procedure.

Interestingly, the final strains along both directions were still tensile after the completion of backfilling. To predict the burial depth at which strains switch from tensile to compressive, a linear equation was chosen to curve fit the strain results starting from 0.5 m height. A minimum burial depth of 2.55 m is determined at which the circumferential strain is zero. This value is derived using the results from Gauge 22 and the associated coefficient of determination R^2 is 0.86.

5.2 Pipe-Wall Strain Profile

To investigate the development of strain profile, the circumferential and longitudinal strains are presented at selected heights from the invert as shown in Figure 8. 0º and 180º refer to the pipe crown and invert, respectively. The springlines are locations at 90º and 270º from the crown. Positive and negative strains are tensile and compressive, respectively.

Similar to those shown in Figure 7, strains at all

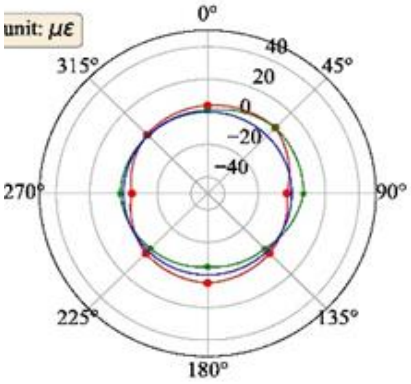

(a) 0.30 m from invert (springline height)

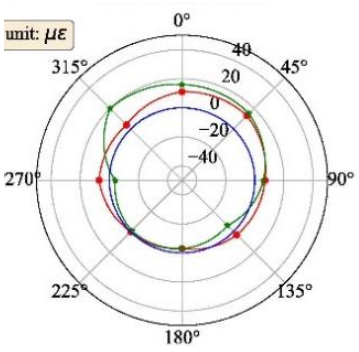

(b) 0.43 m from invert

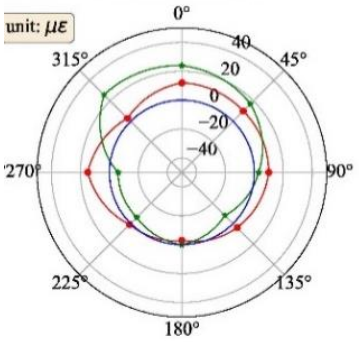

(c) 0.60 m from invert (pipe top level)

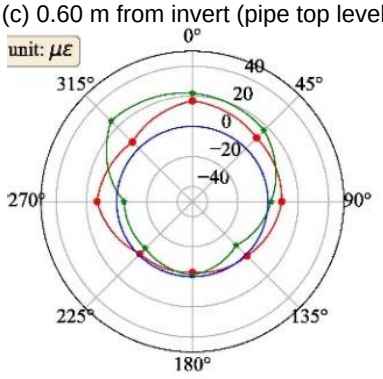

(d) 0.9 m from invert

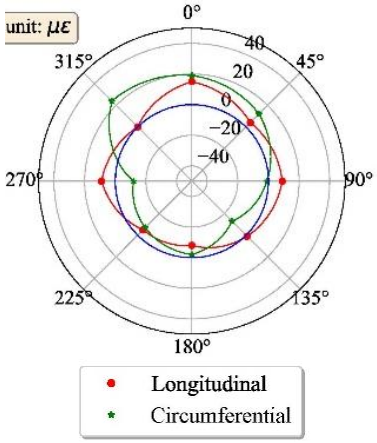

(e) 1.2 m from invert (final depth of cover = 0.6 m)

Figure 8. Pipe-wall strain profiles at Section B at different heights during compaction

locations display an increase in reading, followed by a decrease. The strain profile is generally symmetrical with respect to the vertical diameter. This confirms the uniformity of compaction at two sides of the pipe. With respect to the horizontal diameter, the upper and lower parts of the pipe were under tension and compression in both circumferential and longitudinal directions, respectively. The curvature below the springlines increased as the pipe was supported by haunches, which resulted in the pipe being lifted off the bedding (Chapman et al. 2007). Therefore, only very small readings were recorded at the invert since no pressure was transferred from the soil material. However, when compacting the sidefill material, the pipe ring tended to be laterally contracted, thus the pipe crown became more curved and tensile strains were recorded.

The circumferential to longitudinal strain ratios are generally larger than unity at different locations around the circumference, which means the pipe ring behavior is more significant than the longitudinal bending. This is as expected when the soil material is uniformly distributed along the pipe axis. While significant longitudinal bending stress can be resulted by nonuniform bedding distribution and compaction quality (Jeyapalan et al. 1987, Buco et al. 2006). However, at locations like crown and springlines, the absolute magnitudes of the two strains were close. Therefore, the longitudinal stress could be important and even the maximum stress component.

5.3 Predicted Deformed Shape

Rogers (1988) pointed out that the strain profile is useful in deducing the deformed shape of pipe. In this study, the deformed shape after installation was predicted based on the strain profiles shown in Figure 8. The curvature decreased at the upper part above the springlines but increased at the lower part. Therefore, there exists a point between the shoulder and springline where the strain is zero as indicated by the strain profile. Finally, the deformed pipe ring is determined as an inverted “Y” shape as shown in Figure 9. This so-called inverted “Y” deformation was firstly named by Rogers et al. (1996) when investigating the behavior of plastic pipe during installation.

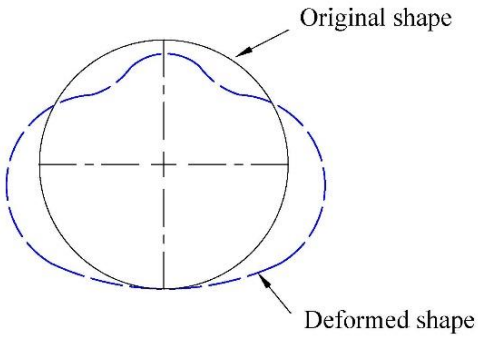

Figure 9. Inverted "Y" deformation (after (Rogers et al. 1996, Fleming et al. 1997))

This deformation is most significant prior to the compaction up to the pipe top level. After that, the pipe crown is flattened under the vertical soil pressure acting right above it. In addition, the highly compacted sidefill can lead to a higher lateral soil reaction at two sides of the pipe than a lightly compacted soil material. Because the reaction modulus of sidefill increases with the relative density (CSA 2014). The magnitude of the lateral soil reaction controls how much the pipe can be re-rounded. This deformed shape is different from that assumed by the well-known Iowa deflection formula (Spangler 1938). The elliptical deformation is assumed to be vertically contracted and horizontally elongated. It applies when flexible pipe is buried in lightly compacted surroundings. However, if the soil at pipe sides is well compacted, prediction of the deformed shape would be more complicated. The diametral deflections and pipe-wall strain profile, one or both of them should be measured to have a reliable prediction. These measurements need to be taken at locations more than just vertical and horizontal vertices. Otherwise, a precise determination of the stress switch zone is very difficult. For example, without measuring the strains at the shoulders and haunches, it is very difficult to distinguish the heart-shaped deformation from the inverted heart-shaped one shown in Figure 1, because the signs of strains at the crown, invert and springlines are the same. For the heart-shaped deformation, a nearly zero strain is expected at the haunches, while a high tensile strain is measured at the shoulders. However, the results are right opposite to this pattern for the inverted heart-shaped deformation. This is due to the difference in curvature change. Therefore, a minimum number of 8 locations, as adopted in this study, is recommended for deflection and strain measurements.

6 SUMMARY AND CONCLUSIONS

Full-scale indoor experiment was conducted on a 24 in. diameter steel pipe to investigate its behavior during installation in a soil pit. Strain gauges were mounted at of two sections at a 1.8 m distance. Measurements of the circumferential and longitudinal strains were taken during the whole process of compaction. The pipe-wall strain profile was illustrated, and the deformed shape was predicted based on the strain profile. Several findings are identified:

(1) The masonry wall is rigid and has very limited impact on the pipe-soil system;
(2) Strains measured at the two instrumented sections were comparable to each other, which confirmed the uniformity of compaction along the pipe axis. In addition, the compaction at both sides of the pipe was confirmed uniform by the symmetry of the pipe-wall strain profile;
(3) During the compaction procedure, both circumferential and longitudinal strains exhibit an increase up to the pipe top level, followed by a decrease due to the placement and compaction of soil above the pipe;

(4) The pipe ring behavior is more important than the longitudinal bending, because the circumferential to longitudinal strain ratio is larger than unity;
(5) The deformed pipe shape is predicted to be an inversed “Y” configuration. A reliable prediction can only be made when the strain or/and deflection readings are recorded at locations other than those at the crown, invert and springlines. At least eight locations along the pipe circumference should be instrumented.

7 ACKNOWLEDGEMENT

The authors wish to thank Enbridge and NSERC (Natural Sciences and Engineering Research Council of Canada) who funded this research. Technical support provided by Donald Anson and Terry Queen at University of Calgary is greatly appreciated.

8 REFERENCES

AASHTO. 1999. AASHTO LRFD Bridge Design Specifications. American Association of State Highway and Transportation Officials.

Alberta Energy Regulator. 2013. Report 2013-B : Pipeline Performance in Alberta, 1990-2012. (August): 1–104.

American Iron and Steel Institute. Highway Task Force. 2007. Handbook of Steel Drainage and Highway Construction Products. American Iron and Steel Institute.

ASTM D2487-11. 2017. Standard Practice for Classification of Soils for Engineering Purposes (Unified Soil Classification System). Annual Book of ASTM Standards. ASTM, International West Conshohocken, PA,: 1–5. doi:10.1520/D2487-11.

Brachman, R.W.I., Moore, I.D., Munro, S.M. 2008. Compaction Effects on Strains within Profiled Thermoplastic Pipes. Geosynthetics International, **15**(2): 72–85. doi:10.1680/gein.2008.15.2.72.

Buco, J., Emeriault, F., Le Gauffre, P., Kastner, R. 2006. Statistical and 3D Numerical Identification of Pipe and Bedding Characteristics Responsible for Longitudinal Behavior of Buried Pipe. Pipelines 2006,: 83–83. doi:10.1061/40854(211)83.

Chapman, D.N., Fleming, P.R., Rogers, C.D.F., Talby, R. 2007. The Response of Flexible Pipes Buried in Sand to Static Surface Stress. Geomechanics and Geoengineering, **2**(1): 17–28. doi:10.1080/17486020601150613.

CSA. 2014. Canadian Highway Bridge Design Code. *In* CSA standard CAN/CSA-S6-00. Canadian Standards Association, Rexdale, Ont.

Fleming, P.R., Faragher, E., Rogers, C.D.F. 1997. Laboratory and Field Testing of Large-Diameter Plastic Pipe. Transportation Research Record, (1594): 208–216. doi:10.3141/1594-24.

Howard, A.K. 1972. Laboratory Load Tests on Buried Flexible Pipe. : 655–662.

Jeyapalan, J.K, Abdel-Magid, B. 1987. Longitudinal Stresses and Strains in Design of RPM Pipes. Journal of Transportation Engineering., **113**(3): 315–331.

Lay, G.R. 2012. Response of Reinforced Concrete and Corrugated Steel Pipes to Surface Load. MSc thesis, Queen’s University (Canada). 1-331.

Lay, G.R., Brachman, R.W.I. 2014. Full-Scale Physical Testing of A Buried Reinforced Concrete Pipe under Axle Load. Canadian Geotechnical Journal, **51**(4): 394–408. doi:10.1139/cgj-2012-0256.

Masada, T., Sargand, S.M. 2007. Peaking Deflections of Flexible Pipe during Initial Backfilling Process. Journal of Transportation Engineering, **133**(2): 105–111. doi:10.1061/(ASCE)0733-947X(2007)133:2(105).

McGrath, T.J., Selig, E.T., Webb, M.C., Zoladz, G. 1999. Pipe Interaction With The Backfill Envelope. U.S Department of Transportation, McLean, VA. 1-274.

Moghaddas Tafreshi, S.N., Khalaj, O. 2011. Analysis of Repeated-Load Laboratory Tests on Buried Plastic Pipes in Sand. Soil Dynamics and Earthquake Engineering, **31**(1): 1–15. doi:10.1016/j.soildyn.2010.06.016.

Nielson, F.D. 1972. Experimental Studies in Soil-Structure Interaction. Highway Research Record, (413): 30–44.

Rogers, C.D.F. 1988. Some Observations on Flexible Pipe Response to Load. Transportation Research Record, **9**(1191): 1–11.

Rogers, C.D.F., Fleming, P.R., Loeppky, M.W.J., Faragher, E. 1995. Structural Performance of Profile-Wall Drainage Pipe - Stiffness Requirements Contrasted with Results of Laboratory and Field Tests. Transportation Research Record, (1514): 83–92.

Rogers, C.D.F., Fleming, P.R., Talby, R. 1996. Use of Visual Methods to Investigate Influence of Installation Procedure on Pipe-Soil Interaction. Transportation Research Record, (1541): 76–85. doi:10.3141/1541-10.

Sargand, S.M., Hazen, G.A., Liu, X., Masada, T., Hurd, J.O. 1995. Structural Performance of Buried Polyvinyl Chloride Pipes under Large Distributed Load. Transportation Research Record, (1514): 59–67.

Spangler, M.G. 1938. The Structural Design of Fexbible Pipe Culverts. Highway Research Board Proceedings, **17**: 235–239.

Terzaghi, K. 1943. Conditions for Shear Failure in Ideal Soils. *In* Theoretical Soil Mechanics. Wiley, New York. 66–76.